Gate Leakage Models for Device Simulation

A. Gehring and S. Selberherr
Institute for Microelectronics, TU Vienna, A-1040 Vienna, Austria
Email: {gehring|selberherr}@iue.tuwien.ac.at

Abstract

The modeling of gate leakage has been of strong interest in recent years, and with the accelerating pace of device miniaturization it is becoming more and important. We outline a detailed survey of tunneling models describing carrier transport through insulating layers suitable for semiconductor device simulation. The crucial topics are separately discussed, comprising models for the energy distribution function, the transmission coefficient for single and layered dielectrics, defect-assisted tunneling and its relation to dielectric degradation and breakdown, and the influence of quasi-bound states in the inversion layer. The models are compared to measurements and commonly used compact models.

1. Introduction

For the prediction of device performance in state-of-the-art semiconductor devices the simulation of quantum-mechanical tunneling effects is of increasing importance. The application area of such models ranges from the prediction of gate leakage in MOS transistors, the evaluation of gate stacks for advanced high-κ gate insulator materials, the optimization of programming and erasing times in non-volatile semiconductor memory cells up to the study of source-drain tunneling. However, tunneling model implementations in state-of-the-art device simulators often rely on simplified models assuming Fermi-Dirac statistics and triangular energy barriers. In miniaturized devices these assumptions are violated in several important aspects. First, the electron energy distribution function (EED) can in general not be described by a Fermi-Dirac or Maxwellian distribution. Higher order moments are necessary to more accurately characterize the distribution of hot carriers [1]. The second weakness lies in the estimation of the transmission coefficient by the WKB or Gundlach method. Energy barriers which are not of triangular or trapezoidal shape are not treated correctly by these models. To accurately describe tunneling in such cases, Schrödinger's equation must be solved. This is usually achieved using the transfer-matrix method [2]. This method, however, is numerically stable only for layer thicknesses up to a few nanometers. We therefore propose to use the quantum transmitting boundary method instead [3].

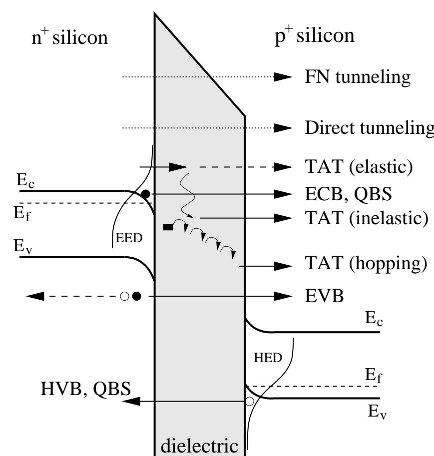

Figure 1. Tunneling processes in an MOS structure.

Finally, an inaccuracy arises when tunneling current from the channel of inverted MOSFETs is calculated. In this case, bound and quasi-bound states are formed, the latter giving rise to quasi-bound state tunneling. The Tsu-Esaki formula, which assumes a continuum of states, cannot be used in this case.

An overview of the different tunneling mechanism is given in Fig. 1. Considering simply the shape of the energy barrier, Fowler-Nordheim (FN) tunneling and direct tunneling can be separated. However, a more rigorous classification distinguishes between ECB (electrons from the conduction band), EVB (electrons from the valence band), HVB (holes from the valence band), TAT (trap-assisted tunneling) processes, and QBS (quasi-bound state) tunneling processes. We denote direct tunneling all processes which are not defect-assisted. In the figure, the electron and hole energy distribution functions are also indicated.

In Section 2, the theory of direct tunneling mechanisms with emphasis on the modeling of the distribution function and the transmission coefficient is outlined. Section 3 describes a set of models which can be used to model defect-assisted tunneling based on inelastic phonon-assisted transitions and related effects such as dielectric degradation and breakdown. Finally, Section 4 describes the calculation of tunneling in the presence of bound and quasi-bound states as encountered in the inversion layer of a MOSFET. A conclusion wraps up the main findings and gives directions for future research.

0-7803-8511-X/04/$20.00 @2004 IEEE.

2. Direct Tunneling

The most prominent and almost exclusively used expression to describe direct tunneling transitions has been developed by Duke [4] and used by Tsu and Esaki to describe tunneling through a one-dimensional superlattice [2]. It is commonly known as Tsu-Esaki expression. The current density reads

$$J = \frac{4\pi m_{\mathrm{eff}} \mathrm{q}}{h^3} \int_{\mathcal{E}_{\min}}^{\mathcal{E}_{\max}} TC(\mathcal{E}_x) N(\mathcal{E}_x) \, \mathrm{d}\mathcal{E}_x \,, \tag{1}$$

with a transmission coefficient $TC(\mathcal{E}_{\mathrm{x}})$ and a supply function $N(\mathcal{E}_{\mathrm{x}})$ which is defined as

$$N(\mathcal{E}_x) = \int_0^{\infty} (f_1(\mathcal{E}) - f_2(\mathcal{E})) \, \mathrm{d}\mathcal{E}_\rho \,. \tag{2}$$

In these expressions the total energy $\mathcal{E}$ is the sum of a transversal component parallel to the Si-SiO_2 interface $\mathcal{E}_\rho$ and a transversal component $\mathcal{E}_x$. The electron energy distribution functions in the gate and substrate are denoted by f_1 and f_2, respectively. It is assumed that the transmission coefficient only depends on the transversal energy component and can therefore be treated independently of the supply function. For a Fermi-Dirac distribution the supply function evaluates to

$$N(\mathcal{E}_{\mathrm{x}}) = \mathrm{k_B} T \ln \left(\frac{1 + \exp\left(-\dfrac{\mathcal{E}_x - \mathcal{E}_{\mathrm{F},1}}{\mathrm{k_B} T}\right)}{1 + \exp\left(-\dfrac{\mathcal{E}_x - \mathcal{E}_{\mathrm{F},2}}{\mathrm{k_B} T}\right)} \right) . \tag{3}$$

where $\mathcal{E}_{\mathrm{F},1}$ and $\mathcal{E}_{\mathrm{F},2}$ denote the Fermi energies at the semiconductor-oxide interfaces. Although this expression is frequently used in the literature, it is not valid to describe hot-carrier tunneling.

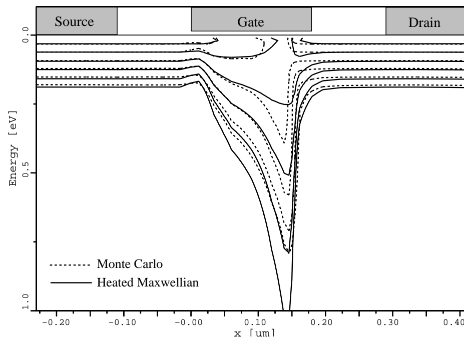

Figure 2. Comparison of the heated Maxwellian distribution (full lines) with the results from a Monte Carlo simulation (dotted lines) in a turned-on 180 nm MOSFET. Neighboring lines differ by a factor of 10.

2.1 Distribution Function Modeling

Models for the EED of hot carriers in the channel region of a MOSFET have been studied by numerous authors [5, 6]. The topic is of high importance because the assumption of a cold Maxwellian distribution function

$$f(\mathcal{E}) = A \cdot \exp\left(-\frac{\mathcal{E}}{\mathrm{k_B} \cdot T_{\mathrm{L}}}\right) , \tag{4}$$

where T_{L} denotes the lattice temperature and A a normalization constant, underestimates the high-energy tail of the EED near the drain region. The straightforward approach is to use a heated Maxwellian distribution function where the lattice temperature T_{L} is simply replaced by the electron temperature T_n. However, the comparison with the results of Monte Carlo simulations in Fig. 2 which shows the contour lines of the heated Maxwellian EED in comparison to Monte Carlo results for a MOSFET with a gate length of L_{g}=180 nm at V_{DS}= V_{GS}= 1 V makes clear that the heated Maxwellian distribution (full lines) yields only poor agreement with the Monte Carlo results (dashed lines). Particularly the high-energy tail near the drain side of the channel is heavily overestimated by the heated Maxwellian model.

A distribution function accounting for the cold carrier population near the drain contact was proposed by Sonoda *et al.* [6], and an improved model has been suggested by Grasser *et al.* [1]:

$$f(\mathcal{E}) = A \left(\exp\left(-\left(\frac{\mathcal{E}}{\mathcal{E}_{\mathrm{ref}}}\right)^b\right) + c \exp\left(-\frac{\mathcal{E}}{\mathrm{k_B} T_{\mathrm{L}}}\right) \right) . \tag{5}$$

The values of $\mathcal{E}_{\mathrm{ref}}$, b, and c are derived from the solution variables of a six moments transport model [1]. Fig. 3 shows the results of this model compared with the Monte Carlo simulations, where an almost perfect agreement can be seen.

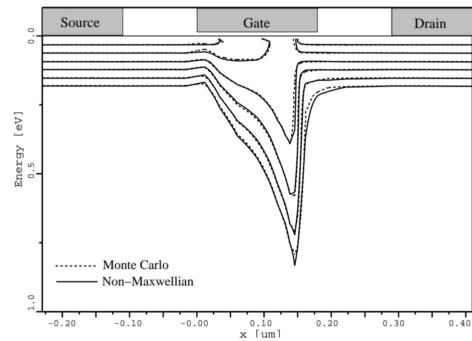

Figure 3. Comparison of the non-Maxwellian distribution (full lines) with the results from a Monte Carlo simulation (dotted lines) in a turned-on 180 nm MOSFET. Neighboring lines differ by a factor of 10.

2.2 Transmission Coefficient Modeling

Apart from the distribution function the quantum-mechanical transmission coefficient is the second building block of any tunneling model. It is based on the probability flux

$$j = \frac{\hbar}{2im} \cdot (\Psi^* \cdot \nabla\Psi - \nabla\Psi^* \cdot \Psi) \qquad (6)$$

where Ψ is the wave function, m the carrier mass, and $i = \sqrt{-1}$. The transmission coefficient is the ratio of the fluxes due to an incident and a reflected wave. These wave functions can be found by solving the stationary one-dimensional Schrödinger equation in the barrier region. This can be achieved using different numerical methods, such as the commonly applied Wentzel-Kramers-Brillouin (WKB) approximation or Gundlach's method [7]. A more general approach is the transfer-matrix method [2] the basic principle of which is the approximation of an arbitrary-shaped energy barrier by a series of barriers with constant or linear potential. Since the wave function for such barriers can easily be calculated, the transfer matrix can be derived by a number of subsequent matrix computations. From the transfer matrix, the transmission coefficient can be calculated. However, the main shortcoming of the method is that it becomes numerically instable for thick barriers which is due to the multiplication of exponentially growing and decaying states, leading to rounding errors which eventually exceed the amplitude of the wave function itself [8]. An alternative method to compute the transmission coefficient is based on the quantum transmitting boundary method [9, 3]. The method uses a finite-difference approximation of Schrödinger's equation with open boundary conditions. This results in a complex-valued linear equation system for the unknown values of the wave amplitudes.

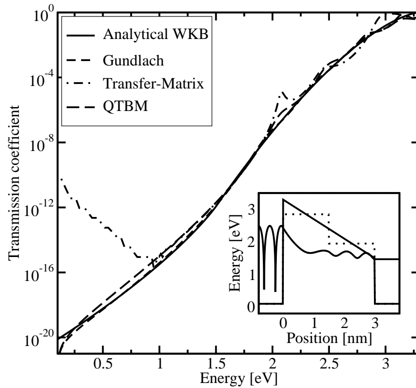

Figure 4. The transmission coefficient using different methods for a dielectric consisting of a single layer. The shape of the energy barrier and the wave function at 2.8 eV is shown in the inset.

Fig. 4 shows the transmission coefficient for a triangular energy barrier with the energy barrier and the values of $|\Psi|^2$ at $\mathcal{E} = 2.8\,\text{eV}$ in the inset. The numerical instability of the transfer-matrix method leads to an increasing transmission coefficient for energies below 1 eV. The Gundlach and analytical WKB methods deliver similar results for the triangular barrier, however, the WKB method does not resolve oscillations in the transmission coefficient. The transmitting boundary method delivers the same results as the Gundlach method which provides an accurate analytical solution in this case [10].

2.3 Comparison with Measurements

The Tsu-Esaki model with an analytical WKB transmission coefficient is in good agreement with measured data for devices with different gate lengths and bulk doping as shown in Fig. 5 for nMOS (top) and pMOS devices (bottom) [11]. The simulations in this figure have been performed using the device simulator MINIMOS-NT [12]. It can be seen that the gate current density can be reproduced over a wide range of dielectric thicknesses with a single set of physical parameters. Note, however, that the assumption of a constant electron mass in the dielectric may no more be justified for ultrathin SiO_2 layers but must be replaced by an energy-dependent mass [13].

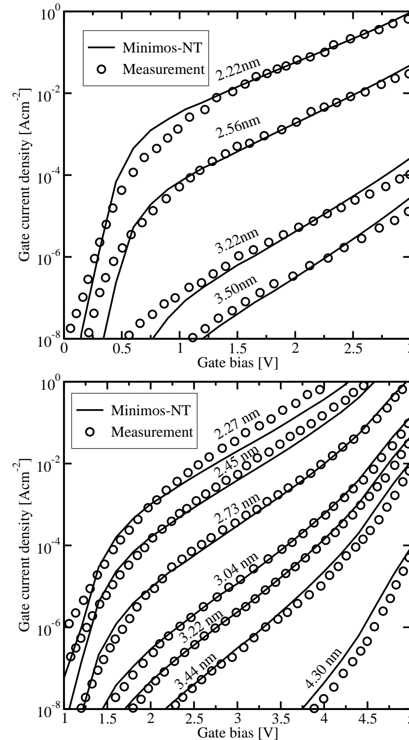

Figure 6. Comparison of the gate current predicted by the Tsu-Esaki model with measurements of an nMOS (top) and a pMOS (bottom) transistor [11].

2.4 Compact Models

For the use in practical device simulation it is desirable to use compact models which do not require large computational resources. The most commonly used model to describe tunneling is the Fowler-Nordheim formula [14]:

$$J = \frac{\mathrm{q}^3 m_\mathrm{eff}}{8\pi m_\mathrm{ox} h \mathrm{q}\Phi_\mathrm{B}} E_\mathrm{ox}^2 \exp\left(-\frac{4\sqrt{2m_\mathrm{ox}(\mathrm{q}\Phi_\mathrm{B})^3}}{3\hbar \mathrm{q} E_\mathrm{ox}}\right) . \tag{7}$$

This expression is not valid for direct tunneling where the barrier is of trapezoidal shape. Schuegraf and Hu derived correction terms for this expression to make it applicable to the regime of direct tunneling [15]

$$J = \frac{\mathrm{q}^3 m_\mathrm{eff}}{8\pi m_\mathrm{ox} h \mathrm{q}\Phi_\mathrm{B} B_1} E_\mathrm{ox}^2 \exp\left(-\frac{4\sqrt{2m_\mathrm{ox}(\mathrm{q}\Phi_\mathrm{B})^3} B_2}{3\hbar \mathrm{q} E_\mathrm{ox}}\right) , \tag{8}$$

For a triangular barrier the correction factors become $B_1 = B_2 = 1$ and the expression simplifies to (7). The compact tunneling models are compared in Fig. 7 for an nMOS structure with 3 nm dielectric thickness. The Schuegraf model fails to describe the tunneling current density at low bias. For high bias, however, it may be used to provide an estimation of the gate current. The Fowler-Nordheim model totally fails for this low electric field. Furthermore, the Fowler-Nordheim model shows the minimum gate current at minimum electric field in the dielectric, and not for the minimum gate bias.

3. Defect-Assisted Tunneling

Shrinking of gate dielectric thicknesses demands the use of alternative gate dielectrics such as ZrO_2. These materials, however, suffer from high defect densities [16]. Therefore, gate dielectric reliability becomes a crucial issue. Defect-assisted gate leakage is frequently described by inelastic trap-assisted tunneling transitions [17].

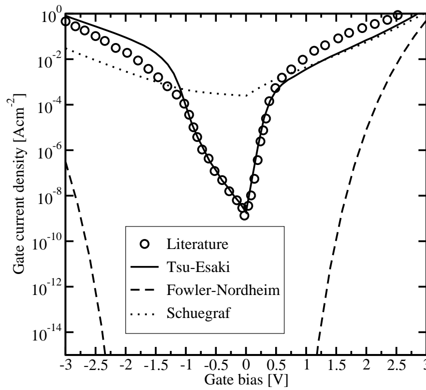

Figure 7. Comparison of different compact models with the Tsu-Esaki model for an nMOS structure [18].

Fig. 8 shows the basic trap-assisted tunneling process through the gate dielectric. Electrons are captured from the cathode, relax to the energy of the trap $\mathcal{E}_0$ by phonon emission with energy $m\hbar\omega$, and are emitted to the anode. The trap-assisted tunneling current is found by integration over the dielectric thickness

$$J_\mathrm{t} = \mathrm{q} \int_0^{t_\mathrm{diel}} \frac{N_\mathrm{T}(x)}{\tau_\mathrm{c}(x) + \tau_\mathrm{e}(x)} \mathrm{d}x, \tag{9}$$

where $N_\mathrm{T}(x)$ is the trap concentration and $\tau_\mathrm{c}(x)$ and $\tau_\mathrm{e}(x)$ denote the capture and emission times calculated from

$$\tau_\mathrm{c}^{-1}(z) = \int_{\mathcal{E}_0}^{\infty} c_n(\mathcal{E}, x) T_\mathrm{l}(\mathcal{E}) f_\mathrm{l}(\mathcal{E})\, \mathrm{d}\mathcal{E} , \tag{10}$$

$$\tau_\mathrm{e}^{-1}(z) = \int_{\mathcal{E}_0}^{\infty} e_n(\mathcal{E}, x) T_\mathrm{r}(\mathcal{E})(1 - f_\mathrm{r}(\mathcal{E}))\, \mathrm{d}\mathcal{E} . \tag{11}$$

In these expressions, c_n and e_n denote the capture and emission rates, f_l and f_r the Fermi distributions, and T_l and T_r the transmission coefficients from the left and right side of the dielectric. The capture and emission processes are described by their respective probabilities which can be calculated by assuming constant [19] or energy-dependent capture cross sections [20], and the transmission coefficients were evaluated by the WKB method. While the neutral defects cause trap-assisted tunneling and gate leakage, only the occupied traps lead to threshold voltage degradation and wearout of the gate dielectric, modeled by a space charge $\rho(x) = Q_\mathrm{T} N_\mathrm{T}(x) f_\mathrm{T}(x)$ in the Poisson equation, where f_T denotes the trap occupancy and Q_T the trap charge state [21].

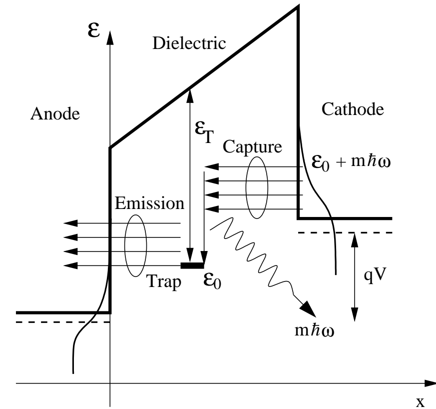

Figure 8. Trap-assisted tunneling transition by inelastic phonon emission. Electrons are captured from the cathode, relax to the trap energy level $\mathcal{E}_0$ by the emission of phonons, and are emitted to the anode.

The neutral defects create percolation paths in the dielectric, which eventually connect the gate with the substrate [22]. In MINIMOS-NT the traps are placed randomly, and the defect concentration N_T is assumed to be proportional to the total injected charge Q_i via $N_\mathrm{T} = CQ_\mathrm{i}^\alpha$ as proposed by Degraeve *et al.* [23], who found values of $C = 5.3\times10^{-19}\,\mathrm{cm}^{-1.88}\mathrm{As}^{-0.56}$ and $\alpha = 0.56$ for dielectric thicknesses between 7.3 and 13.8 nm. As soon as a percolation path through the dielectric is created, the dielectric layer loses its insulating behavior.

To predict the transient behavior of fast switching processes, the charging and decharging dynamics of the traps must be considered. The concentration of occupied traps at position x and time t is generally described by

$$N_\mathrm{T}(x)\frac{\mathrm{d}f_\mathrm{T}(x,t)}{\mathrm{d}t} = N_\mathrm{T}(x)\frac{1-f_\mathrm{T}(x,t)}{\tau_\mathrm{c}(x,t)} - N_\mathrm{T}(x)\frac{f_\mathrm{T}(x,t)}{\tau_\mathrm{e}(x,t)}$$

where τ_c and τ_e describe the capture and emission time of the trap. For the stationary case, the time derivative on the left-hand side is zero and the expression (9) can be derived, while for the transient case, the time constants must be evaluated in each time step. The occupancy function can be calculated iteratively by $f_\mathrm{T}(t_i) = A_i + B_i f_\mathrm{T}(t_{i-1})$ where A_i and B_i depend on the capture and emission times at the time step t_i by [21]

$$A_i = \frac{\tau_\mathrm{c}^{-1}(t_i)\Delta t_i}{1+C_i}, \quad B_i = \frac{1-C_i}{1+C_i},$$

$C_i = \tau_\mathrm{m}^{-1}(t_i)\Delta t_i/2$, $\tau_\mathrm{m}^{-1} = \tau_\mathrm{c}^{-1} + \tau_\mathrm{e}^{-1}$, and $\Delta t_i = t_i - t_{i-1}$. Once the time-dependent occupancy function in the dielectric is known, the tunnel current through the left or right interface at time t_i is

$$J_\mathrm{l,r}(t_i) = \mathrm{q}\int_0^{t_\mathrm{diel}} N_\mathrm{T}(x)\tau_\mathrm{l,r}^{-1}(x,t_i)\,\mathrm{d}x \qquad (12)$$

where the time constants τ_l and τ_r are calculated from

$$\tau_\mathrm{l,r}^{-1}(t_i) = \tau_\mathrm{cl,r}^{-1}(t_i) - f_\mathrm{T}(t_i)\left[\tau_\mathrm{cl,r}^{-1}(t_i) + \tau_\mathrm{el,r}^{-1}(t_i)\right]$$

with the respective values of the capture and emission times to the left and right interface $\tau_\mathrm{cl,r}$ and $\tau_\mathrm{el,r}$. Note that the current through the two interfaces is, in general, not equal. Only after the trap charging processes are finished, the capture and emission currents at the interfaces are in equilibrium.

4. Quasi-Bound State Tunneling

Up to now it has been assumed that all energetic states in the substrate contribute to the tunneling current. In the channel of small MOSFETs, however, the high electric field leads to a quantum-mechanical quantization of carriers. If it is assumed that the wave function does not penetrate into the gate, discrete energy levels can be identified. However, it cannot be assumed that electrons tunnel from these energies, since for the derivation of the levels it was assumed that there is no wave function penetration into the dielectric. Taking a closer look at the conduction band edge of a MOSFET in inversion reveals that, depending on the boundary conditions, different types of quantized energy levels must be distinguished. Bound states are formed at energies for which the wave function decays to zero at both sides. Quasi-bound states (QBS) have closed boundary conditions at one side and open boundary conditions at the other side. Free states, finally, are states which do not decay at any side. The Tsu-Esaki equation (1) must therefore be replaced by a formula accounting for quasi-bound state and continuum tunneling

$$J = \frac{\mathrm{k_B}T\mathrm{q}}{\pi\hbar^2}\sum_{i,\nu}\frac{g_\nu m_\parallel}{\tau_\nu(\mathcal{E}_{\nu,i})}\ln\left(1+\exp\left(\frac{\mathcal{E}_\mathrm{F}-\mathcal{E}_{\nu,i}}{\mathrm{k_B}T}\right)\right) + \frac{4\pi\mathrm{q}m_\mathrm{dos}}{h^3}\int_{\mathcal{E}_\mathrm{min}}^{\mathcal{E}_\mathrm{max}} TC(\mathcal{E}_x, m_\mathrm{ox})N(\mathcal{E}_x)\,\mathrm{d}\mathcal{E}_x\,, \qquad (13)$$

where the symbols g_ν and $m_\parallel$ denote the valley degeneracy and parallel masses ($g_\nu = 2$ for $m_\parallel = m_\mathrm{t}$ and $g_\nu = 4$ for $m_\parallel = \sqrt{m_\mathrm{l}m_\mathrm{t}}$), and $\tau_\nu(\mathcal{E}_{\nu,i})$ is the life time of the quasi-bound state $\mathcal{E}_{\nu,i}$. Fig. 9 shows the conduction band edge and the resulting wave functions for two specific eigenvalues in the channel of a MOSFET. Several methods have been reported for the calculation of the life times [24, 25, 3]. However, these methods are computationally demanding and therefore hardly suitable for implementation in a device simulator. Conventional device simulation packages even neglect the QBS tunneling component at all and use only the Tsu-Esaki formula (1) instead.

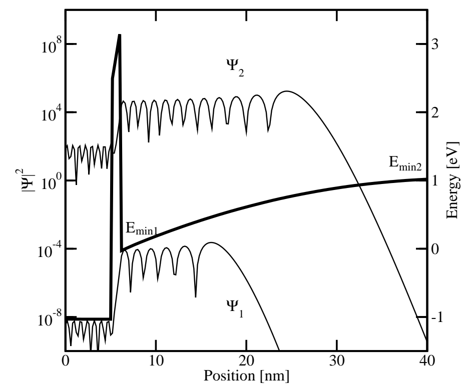

Figure 9. The conduction band profile and two quasi-bound state wave functions.

We propose to use the quasi-classical approach where the life time is calculated from

$$\tau_\nu(\mathcal{E}_{\nu,i}) = \int_0^x \frac{\sqrt{2m_\nu/(\mathcal{E}_{\nu,i} - \mathcal{E}_\mathrm{c}(\xi))}}{TC(\mathcal{E}_{\nu,i})} \,\mathrm{d}\xi \,, \qquad (14)$$

with $\mathcal{E}_\mathrm{c}(x) = \mathcal{E}_{\nu,i}$ [26]. To further reduce the computation time, the QBS tunneling current can be calculated based on the eigenvalues of the triangular well approximation $\mathcal{E}_{\nu,i} = -z_i(\hbar^2/2m_\nu)^{1/3}E^{2/3}$ with z_i being the zeros of the Airy function and E the electric field, instead of calculating the eigenvalues from the complex eigenvalue problem. Since the closed-boundary eigenvalues are higher than their open-boundary pendants, they must be corrected by an empirical fit factor. Thus, an easy and stable formula for the evaluation of quantum and continuum tunneling in CMOS devices is achieved [27].

5. Summary and Conclusion

We presented a hierarchy of tunneling models for semiconductor device simulation. Higher-order transport models are found suitable for the description of hot-carrier tunneling. Common methods to estimate the transmission coefficient of energy barriers have been reviewed and the results were compared to measruements and commonly used compact models. We propose to link an inelastic trap-assisted tunneling model to the occurrence of dielectric wearout and breakdown phenomena in high-κ dielectric materials. Finally, the emergence of quasi-bound states in inverted MOSFETs was discussed. This requires a modification of the Tsu-Esaki formula, and we recommend a method where the life times are calculated based on the eigenvalues of the closed-boundary triangular well approximation. Although these models represent the state-of-the-art at the device simulation level, open questions remain. These comprise the use of a constant effective mass in the dielectric layer, which contradicts *ab-initio* studies, the controversial issue of image force correction, and the modeling of high-κ insulator reliability, which is still in its beginnings.

Acknowledgments

The authors thank Hans Kosina, Tibor Grasser, Francisco Jiménez-Molinos, and Stefan Harasek for valuable contributions throughout this work.

References

[1] Grasser, T., Kosina, H., Heitzinger, C., and Selberherr, S., J.Appl.Phys., 91, pp. 3869–3879 (2002).

[2] Tsu, R. and Esaki, L., Appl.Phys.Lett., 22, pp. 562–564 (1973).

[3] Frensley, W. R., Superlattices & Microstructures, 11, pp. 347–350 (1992).

[4] Duke, C. B., Tunneling in Solids, Academic Press (1969).

[5] Cassi, D. and Riccó, B., IEEE Trans.Electron Devices, 37, pp. 1514–1521 (1990).

[6] Sonoda, K.-I., Yamaji, M., Taniguchi, K., Hamaguchi, C., and Dunham, S. T., J.Appl.Phys., 80, pp. 5444–5448 (1996).

[7] Gundlach, K. H., Solid-State Electron., 9, pp. 949–957 (1966).

[8] Usuki, T., Saito, M., Takatsu, M., Kiehl, R. A., and Yokoyama, N., Physical Review B, 52, pp. 8244–8258 (1995).

[9] Lent, C. S. and Kirkner, D. J., J.Appl.Phys., 67, pp. 6353–6359 (1990).

[10] Gehring, A., Kosina, H., and Selberherr, S., J.Computational Electronics, 2, pp. 219–223 (2003).

[11] Lo, S. H., Buchanan, D. A., and Taur, Y., IBM J.Res.Dev., 43, pp. 327–337 (1999).

[12] Institut für Mikroelektronik, Technische Universität Wien, Austria, MINIMOS-NT 2.0 User's Guide (2002).

[13] Städele, M., Fischer, B., Tuttle, B. R., and Hess, K., Solid-State Electron., 46, pp. 1027–1032 (2002).

[14] Lenzlinger, M. and Snow, E. H., J.Appl.Phys., 40, pp. 278–283 (1969).

[15] Schuegraf, K. F., King, C. C., and Hu, C., in Proc. Symposium on VLSI Technology, pp. 18–19 (1992).

[16] Harasek, S., Wanzenböck, H. D., and Bertagnolli, E., J.Vac.Sci.Technol.A, 21, pp. 653–659 (2003).

[17] Larcher, L., IEEE Trans.Electron Devices, 50, pp. 1246–1253 (2003).

[18] Cai, J. and Sah, C.-T., J.Appl.Phys., 89, pp. 2272–2285 (2001).

[19] Herrmann, M. and Schenk, A., J.Appl.Phys., 77, pp. 4522–4540 (1995).

[20] Jiménez-Molinos, F., Palma, A., Gámiz, F., Banqueri, J., and Lopez-Villanueva, J. A., J.Appl.Phys., 90, pp. 3396–3404 (2001).

[21] Gehring, A., Jiménez-Molinos, F., Kosina, H., Palma, A., Gámiz, F., and Selberherr, S., Microelectron.Reliab., 43, pp. 1495–1500 (2003).

[22] Stathis, J. H., IBM J.Res.Dev., 46, pp. 265–286 (2002).

[23] Degraeve, R., Groeseneken, G., Bellens, R., Ogier, J. L., Depas, M., Roussel, P. J., and Maes, H. E., IEEE Trans.Electron Devices, 45, pp. 904–911 (1998).

[24] Cassan, E., J.Appl.Phys., 87, pp. 7931–7939 (2000).

[25] Clerc, R., Spinelli, A., Ghibaudo, G., and Pananakakis, G., J.Appl.Phys., 91, pp. 1400–1409 (2002).

[26] Dalla Serra, A., Abramo, A., Palestri, P., Selmi, L., and Widdershoven, F., IEEE Trans.Electron Devices, 48, pp. 1811–1815 (2001).

[27] Gehring, A. and Selberherr, S., in Proc. Intl. Conf. on Simulation of Semiconductor Processes and Devices, pp. 25–28, München (2004).